ELSEVIER

International Journal of Mass Spectrometry 223–224 (2003) 217–227

International Journal of Mass Spectrometry

www.elsevier.com/locate/ijms

Effect of temperature on dissociative electron attachment to CCl_2F_2

J.D. Skalny[a,*], S. Matejcik[a], T. Mikoviny[a], T.D. Märk[a,b]

[a] *Department of Plasma Physics, Comenius University, Mlynska dolina, F-2, 842 48 Bratislava, Slovak Republic*
[b] *Institut für Ionenphysik, Technikerstr. 25, A6020 Innsbruck, Austria*

Received 15 January 2002; accepted 4 April 2002

Abstract

Using previously measured relative attachment cross-section functions for freon CCl_2F_2 (at different gas temperatures) we have calculated corresponding absolute attachment cross-section functions with help of a recently devised normalisation procedure involving the use of measured absolute thermal rate constant (and its temperature dependence). Based on these absolute cross-section functions, we have then calculated from these data sets absolute thermal rate constants (for the different gas temperatures) and by using Arrhenius type plots derived corresponding activation energies, which appear to lie below values obtained in swarm experiments. Finally, we have used these absolute cross-section functions to calculate absolute attachment rate constants as a function of mean electron energy $\langle\varepsilon\rangle$ involving four different electron energy distribution functions and have compared the results with available experimental data. Characteristic discrepancies between different data sets are discussed. (Int J Mass Spectrom 223–224 (2003) 217–227)

Keywords: Electron attachment; Freon; Cross-section; Activation energy; Temperature dependence

1. Introduction

The study of the effects of the gas temperature on electron attachment to chlorofluoroalkanes (CFC) is of intrinsic as well of practical interest. It provides information about important thermo-chemical data, i.e., it allows us to determine the activation energy AE for electron attachment. From a practical view, knowledge about the influence of the gas temperature on electron attachment processes is important for a better understanding of electron–molecule interactions in discharge plasmas. Data characterising electron attachment at enhanced or at lowered gas temperatures are necessary for the modelling of processes being active in plasma-chemical technologies. Typical examples of these are the plasma etching processes used in the modern semiconductor technologies, the scrubbing of organic pollutants exhausted from various technological processes or even the circuit breakers, where some of the CFC gases are used like an insulating medium.

Regarding CCl_2F_2 (R-12) there is another reason for this interest resulting from the presence of a relatively large amount of R-12 in the stratosphere. It has been recognised that CCl_2F_2 is a precursor of very efficient catalytic reactions leading to the depletion of ozone in the stratosphere [1]. The dissociative electron attachment to CCl_2F_2 is potential mode of

* Corresponding author. E-mail: skalny@fmph.uniba.sk

1387-3806/02/$ – see front matter © 2002 Published by Elsevier Science B.V.
PII S1387-3806(02)00792-3

its decomposition, which can also initiate sequential processes leading to ozone destruction. According to current models [1], only photodissociation of CCl_2F_2 in the stratosphere is being considered, whereas the role of the dissociative electron attachment has not yet been taken into account in models aimed to describe the depletion of the ozone layer protecting the earth from harmful UV radiation. Because of this potential role in the atmosphere many experiments using both, beams and swarm techniques, have been carried out on electron attachment to CCl_2F_2 the past decades.

A considerable body of data on rate constants as well as cross-section data is today available for electron attachment to CCl_2F_2 [2–36]. Most of the previous studies have been reviewed recently [37], some of the studies also in [38,39]. There are, however, relatively few of them in which electron attachment is studied as a function of both, electron energy and the temperature of the target CCl_2F_2 molecule [6,7,12,15,20–25]. Mostly the thermal rate constant k_{th} (a typical swarm parameter) was determined by various techniques at elevated [6,12,15,22] or even at lowered gas temperature [23]. Very little has been reported on the temperature effect of the electron attachment cross-section. To the authors' knowledge there exist only three recently published papers [20,21,24] and one submitted for publication [41], determining the temperature dependence of the electron attachment cross-section for the process:

$$e^- + CCl_2F_2 \rightarrow Cl^- + CClF_2 \quad (1)$$

It is necessary to note that there exists a frequently mentioned pioneering study by Chen and Chantry [7], however, their results were presented only in form of a short conference abstract. Only some basic data, activation energy AE = 130 meV and the $\sigma(\langle\varepsilon\rangle)$ value at ambient temperature, are available in this abstract, not sufficient for a reliable comparison with the three sets of mentioned experimental results [20,21,24].

Using previously measured relative attachment cross-section functions for freon CCl_2F_2 (at different gas temperatures), we have calculated corresponding absolute attachment cross-section functions with help of a recently devised normalisation procedure involving the use of measured absolute thermal rate constant. Based on these absolute cross-section functions we have then calculated from these data sets absolute thermal rate constants (for the different gas temperatures) and by using Arrhenius type plots derived corresponding activation energies. Finally, we have used these absolute cross-section functions to calculate absolute attachment rate constants as a function of mean electron energy $\langle\varepsilon\rangle$ involving four different electron energy distribution functions and have compared the results with available experimental data. Characteristic discrepancies between different data sets are discussed.

2. Determination of absolute cross-section data from crossed-beams experiments

Swarm experiments provide reliable data characterising the dissociative electron attachment process, either by measured density-reduced electron attachment coefficients η/N or by measured total electron attachment rate constants k [37]. Both parameters are usually expressed as a function of the mean electron energy $\langle\varepsilon\rangle$, and fully describe the collective interaction of an electron cloud characterised by a specific electron energy distribution function (EEDF) with the molecules. Therefore these data are frequently used in models describing the kinetics of technologically interesting, complex processes concerning the generation or the destruction of selected compounds in discharge plasmas.

In contrast to swarm techniques, highly sophisticated beam techniques were developed and are used to study electron interactions with the target atom or molecule under single collision conditions. These studies provide the cross-section relevant to the process under study as a function of the electron energy ε, i.e., $\sigma = f(\varepsilon)$. However, it must be pointed out, that usually only relative data are obtained by those beam techniques. This statement is valid especially for so-called crossed-beams experiments used recently for the determination of the electron attachment cross-section to CCl_2F_2 [21,24,40,41]. The relative data are usually presented as the electron energy

dependent anion yield $Y(\varepsilon)$. In order to obtain absolute values for the cross-section $\sigma(\varepsilon)$, the measured $Y(\varepsilon)$ data are normalised by various techniques [42–45]. Some of these are discussed in [46], and especially in [40,47]. In our earlier paper [21], the simple formula:

$$k_{th} = \sigma(\{\varepsilon\})\{v\} \quad (2)$$

was used for calibration of relative data. The value of the thermal rate constant k_{th}, determined at an ambient temperature of gas T_G, was taken from a swarm experiment [15] in which electrons were in thermal equilibrium with buffer and attaching gas molecules. In the formula (2), $\sigma(\{\varepsilon\})$ is the value of the attachment cross-section corresponding to the electron energy $\{\varepsilon\} = k_B T_e$ and $\{v\}$ is the mean, or median electron velocity at the temperature $T_e = T_G$. The mean or median velocity is defined in accordance with Boltzmann by:

$$\{v\} = \sqrt{\frac{8k_B T_e}{\pi m_e}} \quad (3)$$

Furthermore, it was assumed that the value $\sigma(\varepsilon)$ is directly proportional to the ion yield $Y(\varepsilon)$ detected at the electron energy ε (mono-energetic beam of electrons), i.e.,

$$\sigma(\varepsilon) = CY(\varepsilon) \quad (4)$$

Then for the value $Y(\{\varepsilon\})$ measured at the electron energy $\{\varepsilon\}$ the same expression is valid

$$\sigma(\{\varepsilon\}) = C\,Y(\{\varepsilon\}) \quad (5)$$

The normalisation factor C was obtained from the experimental data for the ion yield at $T_e = 300\,K$ by using Eqs. (2) and (5). Subsequently, the absolute cross-section data, measured at ambient as well as elevated CCl_2F_2 gas temperature, were calculated by multiplying the experimentally measured data of the $Y(\varepsilon)$ by the same normalisation factor C. In principle, the validity of such a procedure involves the assumption that the EEDF in the swarm experiment, which serves as a source of k_{th}, has a Maxwell–Boltzmann shape. Moreover, discrimination effects in the ion extraction process and the transmission of the mass-spectrometer have not been taken into account [40]. Furthermore, it is necessary to note that the reliability of this normalisation procedure ultimately relies on the accuracy of the attachment rate constant k_{th} used. Only if the Cl^- anion produced via (1) is the dominating ion both, in the single collision beams experiments and in the multi-collisions swarm experiments, the k_{th} may be used for the normalisation procedure.

Nevertheless, a recent detailed analysis [40] of this normalisation procedure has revealed that the reliability of results obtained is substantially influenced by the shape of $\sigma(\varepsilon)$. Eqs. (2) and (5) can only be used for this normalisation if the electron energy distribution function in the swarm experiment is a Maxwell–Boltzmann one and the cross-section $\sigma(\varepsilon)$ is either inversely proportional to the electron energy $\sigma \approx \varepsilon^{-1}$ or does not depend on ε at all, i.e., σ = constant. These conditions are, however, seldom met in a specific situation.

Therefore, our earlier data were revised in line with the recent considerations and conclusions reported in [40]. The new absolute attachment cross-section for CCl_2F_2 were determined in [40] by using a procedure similar to one used by Illenberger and Niehaus for an absolute normalisation of relative data concerning total Penning ionisation cross-section [42]. Assuming that (i) the values of the absolute attachment cross-section are directly proportional to the measured yield of ions $Y(\varepsilon)$ and (ii) that electrons are thermalized in the experiment from which the value of k_{th} was taken, then in accordance with [42] the following expression holds:

$$k_{th} = \sqrt{\frac{8}{\pi m_e}} \int_0^\infty CY(\varepsilon)\{\varepsilon\}^{-3/2} \varepsilon \exp\left[\frac{-\varepsilon}{\{\varepsilon\}}\right] d\varepsilon \quad (6)$$

In Eq. (6), the normalised Maxwell–Boltzmann electron energy distribution function has been used. From the $Y(\varepsilon)$ values reported in [21], at $T_e = 300\,K$, the proportionality factor C was derived by numerical integration of Eq. (6). For the normalisation procedure the value $k_{th} = 1.77 \times 10^{-9}\,cm^3\,s^{-1}$, recommended by Christophorou et al. [37] was used for the calculation of C. The same proportionality factor C was then employed for the calculation of the absolute $\sigma(\varepsilon)$ dependencies at other temperatures in the range from

303 to 423 K reported in [21]. A similar procedure was applied to the recently published relative data $\sigma(\varepsilon)$ at elevated temperatures 350–700 K [24] and to the unpublished data of Matejčík et al. obtained at temperatures 402–515 K [41]. For the normalisation of the data in [24], the constant C was determined at $T = 350$ K, using a value of $k_{th} = 3.75 \times 10^{-9}$ cm^3 s^{-1} at $T = 350$ K obtained from an Arrhenius plot $k_{th} = f(1/T)$ using k_{th} (300 K) from above and an $E_A = 136$ meV from [25]. In a similar manner, a value of $k_{th} = 6.72 \times 10^{-9}$ cm^3 s^{-1} at $T = 402$ K was derived for the normalisation of the relative data of Matejčík et al. [41] (obtained at a resolution (FWHM) of about 60 meV). Before the normalisation procedure the experimentally measured yields of ions were corrected for changes in the density of the neutral gas beam with temperature [41].

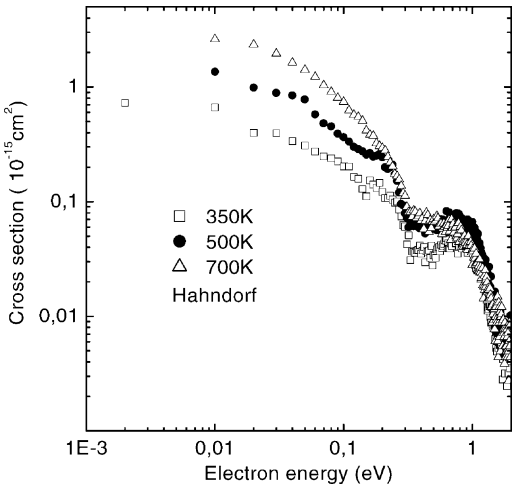

Fig. 2. Temperature dependence of the presently calibrated dissociative electron attachment cross-section for CCl_2F_2 measured in a crossed-beam experiment [24].

3. Results and discussion

Figs. 1–3 display in a log log fashion the electron energy dependent absolute attachment cross-sections data $\sigma(\varepsilon)$ for the process (1) obtained from the relative data [21,24,41] at various temperatures of CCl_2F_2 molecules. A possible discrimination effect, for the extraction of the Cl^- ions into the mass spectrometer was not considered in the present normalisation procedure. The data in Fig. 1 constitute revised data published earlier by Kiendler et al. [21], whereas the absolute cross-section data shown in Fig. 2 are normalised here from the earlier published relative

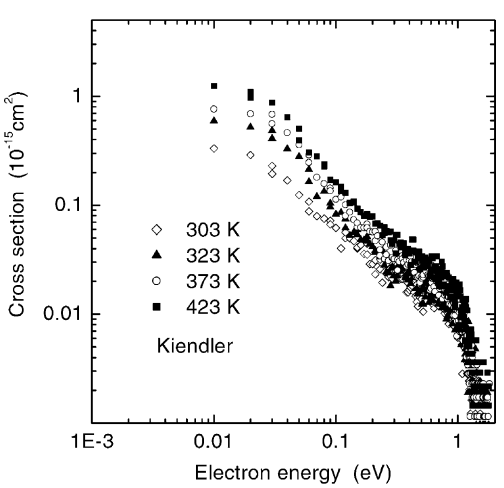

Fig. 1. Temperature dependence of the presently calibrated dissociative electron attachment cross-section for CCl_2F_2 measured in a crossed-beam experiment [21].

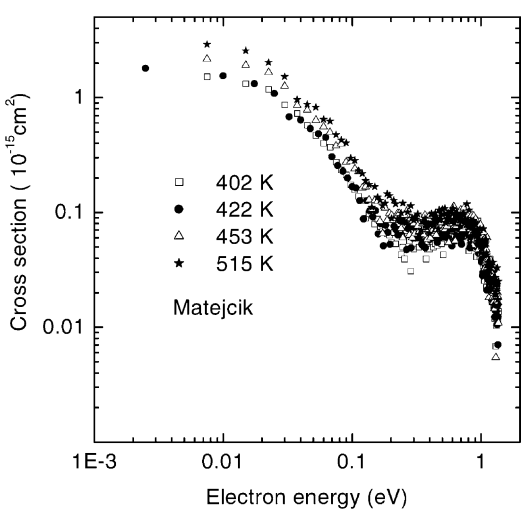

Fig. 3. Temperature dependence of the presently calibrated dissociative electron attachment cross-section for CCl_2F_2 measured in a crossed-beam experiment [41].

cross-section data of Hahndorf and Illenberger [24]. The absolute cross-section data shown in Fig. 3 were obtained from recently measured, not yet published, relative data of Matejčík et al. [41]. The revised data displayed in Fig. 1 are slightly shifted towards smaller values in comparison to the earlier data, which were obtained by using formula (2) and (5) for the conversion of relative to absolute cross-section data [21]. The explanation why only a slight difference is found between the two sets of absolute cross-sections data, using the same k_{th} for normalisation, follows from recently theoretical considerations [40]. It can be seen in Figs. 1–3 that the smaller the electron energy the larger is the dependence on temperature. In contrast to these three measurements shown in Figs. 1–3, the cross-section data reported by Underwood-Lemons et al. do not exhibit any temperature dependence, especially at low electron energy [20]. Moreover, the absolute value of the cross-section maximum of Underwood-Lemons et al. is evidently smaller than the presently obtained values given in Figs. 1–3.

The absolute cross-section data shown in Figs. 1–3, as well as earlier published absolute data $\sigma(\varepsilon)$ [20], were used in the next step for the calculation of the temperature dependence of the thermal value of electron attachment rate constant k_{th}. Moreover, the dependencies of the attachment rate constant k_T, on the mean electron energy at different temperatures of CCl_2F_2 molecules were also calculated. For these calculation the normalised Maxwell–Boltzmann EEDF was used:

$$k_{th} = \sqrt{\frac{8}{\pi m_e}} \int_0^\infty \sigma(\varepsilon)\{\varepsilon\}^{-3/2}\varepsilon \exp\left[\frac{-\varepsilon}{\{\varepsilon\}}\right] d\varepsilon \qquad (7)$$

where $\sigma(\varepsilon)$ corresponds to the electron energy $\{\varepsilon\} = k_B T_e = k_B T_G$ at the gas temperature T_G. In Fig. 4, all four sets of calculated values of electron attachment rate constant are shown along with all earlier published data obtained directly by various swarm techniques. The corresponding Arrhenius plot data shown in Fig. 5 include also the experimental results presented in [7,12]. Since the individual $k_{th}(T_G)$ data originally measured by these authors were not reported (only AE and $k_{300\,K}$ values are available in

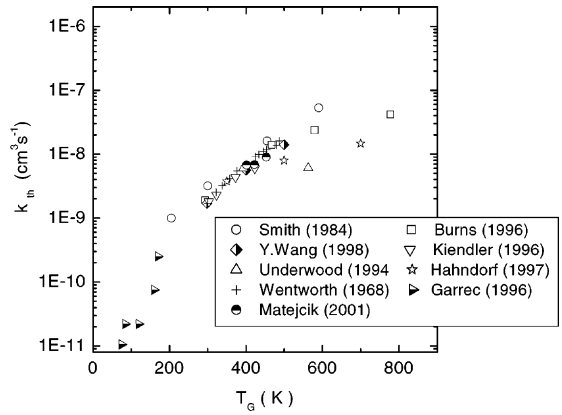

Fig. 4. Variation of the thermal value k_{th} of the dissociative electron attachment constant for CCl_2F_2 with temperature.

[7,12]), the Arrhenius formula:

$$k_{thx} = k_{th} \exp\left\{\frac{AE(T_x - T_{th})}{k_B T_x T_{th}}\right\} \qquad (8)$$

was used for calculation of one value k_{thx} at selected temperature T_x required for drawing $k_{th} = f(1/T)$ plots shown in Fig. 5.

Over the entire temperature range all k_{th} values increase with increasing gas temperature except the results derived from the absolute attachment cross-section data for CCl_2F_2 obtained with a transmission

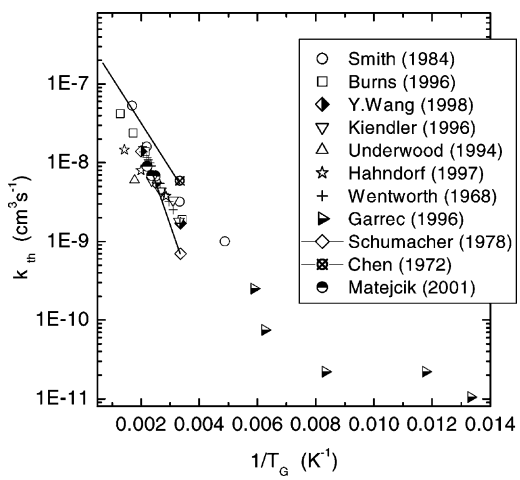

Fig. 5. Arrhenius plot of the dissociative attachment rate constant k_{th} for CCl_2F_2 vs. $1/T_G$.

spectrometer by Underwood-Lemons et al. [20]. There are two sources of systematic errors mentioned by Underwood-Lemons et al. in determining the absolute magnitude of the cross-section in their experiments, the length of the electron trajectory and the target number density. These could be a source of considerable uncertainty in the determining the attachment cross-section.

The AE data determined from Arrhenius plots presented in Fig. 5 are listed in Table 1 together with k_{th} values and important information relating to experimental conditions. The scatter between the different AE values is large (up to a factor of two). Even more conspicuous is the variation of k_{th} (up to an order of magnitude) at room temperature presented in Table 1. As it was concluded recently [22], the spread in

Table 1

k ($cm^3\,s^{-1}$)	T (K)	Method and comments	Reference
Directly measured attachment rate constants			
1.36×10^{-9}	298	Microwave conductivity-pulse radiolysis technique CCl_2F_2 in propane	[9]
8.3×10^{-10}	300	ECR, CCl_2F_2 in Ar or N_2	[8]
1.7×10^{-9}	Room	Pulsed Townsend technique, CCl_2F_2 in Ar or N_2, $k_{th} = f(\langle\varepsilon\rangle)$ up to $\langle\varepsilon\rangle = 5$ eV	[17]
3.2×10^{-9}	300	FALP, CCl_2F_2 in He + Ar, $k_{th} = f(T)$ 205 K $< T <$ 590 K, AE = 0.11 eV	[15]
7.0×10^{-10}	298	ECR, CCl_2F_2 in Ar, $k_{th} = f(T)$ 293 K $< T <$ 453 K, AE = 0.195 eV	[12]
1.8×10^{-9}	Room	Electron cyclotron resonance, CCl_2F_2 in He + Ar	[18]
1.66×10^{-9}	298	Pulsed Townsend techniques, CCl_2F_2 in N_2, $k_{th} = f(T)$ 298 K $< T <$ 550 K, $k_{th} = f(\langle\varepsilon\rangle)$ up to $\langle\varepsilon\rangle$ 1 eV, AE = 0.136 eV (determined using the data from Table II in [25])	[25]
2.0×10^{-10}	170	CRESU (supersonic flow combined with Langmuir probe), $k_{th} = f(T)$ 48 K $< T <$ 170 K, CCl_2F_2 in N_2 (He), AE = 0.073 eV assessed from Arrhenius plot (Fig. 11 in [23]) from only three points at highest temperatures	[23]
Attachment rate constants derived			
1.9×10^{-9}	293	ECR, CCl_2F_2 in He, results calibrated to SF_6, $k_{th} = 2.2 \times 10^{-7}\,cm^{-3}\,s^{-1}$ [48–50], $k_{th} = f(T)$ 293 K $< T <$ 777 K, AE = 0.129 eV (from Fig. 3 in [22])	[22]
5.9×10^{-9}	300	Calculated from attachment cross-section [7] by Smith et al., AE = 0.13 eV, 300 K $< T <$ 1000 K	[15]
2.7×10^{-9}	Room	Estimated by Skalny from data in Fig. 5 [53]	
1.7×10^{-9}	300	Calculated from data in [6] by Smith, AE = 0.147 eV, electron capture coefficient = $f(T)$, 300 K $< T <$ 487 K [6]	[15]
1.23×10^{-9}	298	Calculated from pressure-reduced electron attachment coefficient (αw) data in [13] by Christophorou	[37]
1.0×10^{-9}	298	Calculated from pressure-reduced electron attachment coefficient data in [10] by Smith, $(\alpha w) = f(\langle\varepsilon\rangle)$ up to $\langle\varepsilon\rangle$ =1.0 eV [10]	[15]
1.9×10^{-9}	298	Calculated from the pressure-reduced electron attachment coefficient data in [11] by Christophorou $(\alpha w) = f(\langle\varepsilon\rangle)$ up to $\langle\varepsilon\rangle = 1.0$ eV [11]	[37]
4.0×10^{-10}	300	Calculated from the relative density-reduced electron attachment coefficient data η_{red} in [3] by Smith $\eta_{red} = f(\langle\varepsilon\rangle)$ up to $\langle\varepsilon\rangle$ =1.2 eV [3]	[15]
6.0×10^{-10}	300	Calculated from the cross-section data in [2] by Smith	[15]
1.2×10^{-9}	300	Calculated from the maximum of the cross-section value at an electron energy $\langle\varepsilon\rangle$ = 0.15 eV [4] by Smith	[15]
1.23×10^{-9}	300	Determined from the pressure-reduced electron attachment coefficient data in [13] by Christophorou et al., energy integrated attachment cross-section $\int_{\kappa}^{2.5\,eV} \sigma_a(\varepsilon)d\varepsilon = f(\kappa)$	[14]
9.6×10^{-10}	295	Determined from electron swarm data [27] by Christophorou	[37]
3.6×10^{-9}		Estimated from asymptotic form of cross-section in [16] at the electron energy $\langle\varepsilon\rangle$ = 20 meV	[38]
Recommended values of electron attachment constant k_{th}			
1.0×10^{-9}	300		[38]
1.77×10^{-9}	300	$k_{th} = f(\langle\varepsilon\rangle)$ up to $\langle\varepsilon\rangle$ 5 eV see Fig. 22 in paper [37]	[37]

results does not stem only from systematic differences among used experimental methods, it appears to reflect also uncertainties inherent in electron attachment kinetics measurements. Moreover, below the temperature of 120 K the k_{th} values measured by Le Garrec et al. [23] deviate strongly from the expected linear Arrhenius plot behaviour and are not displayed in Fig. 5.

In contrast to the large scatter of k_{th}, the scatter in AE values is not so dramatic within the temperature range of 300–1000 K. For instance the value of AE = 0.086 eV determined from the experimental values k_{th} within the temperature range of 120–170 K by Le Garrec et al. [23] is identical with the value AE = 0.082 eV derived from the data of Handorf and Illenberger [24].

Figs. 4 and 5 show that there is a good agreement between the experimental k_{th} data [6,22,25] and data calculated from normalised cross-sections [21,41]. Moreover, the data of [21,41] are in fair agreement with the Smith's data [15] except of linear a shift between them. The shift corresponds to the difference between thermal rate constant at 300 K used for normalisation procedure $1.77 \times 10^{-9}\,cm^3\,s^{-1}$ [37] and the value $3.2 \times 10^{-9}\,cm^3\,s^{-1}$ reported by Smith et al. [15]. There is an excellent agreement between earlier data published by Wentworth et al. [6] and recent measurements performed in N_2 seeded with traces of CCl_2F_2 [25]. Also the data obtained by Burns et al. [22] agree with the former two sets of experimental data within the mentioned uncertainties of these experiments. However, this agreement is problematic, because the k_{th} values published by Burns et al. [22] were originally calibrated to an attachment rate constant $2.2 \times 10^{-7}\,cm^3\,s^{-1}$ [48–50] valid for SF_6. If however, the value $k_{th} = 3.1 \times 10^{-7}\,cm^3\,s^{-1}$ published by Smith et al. [15] is applied in the calibration, the values of electron attachment constant for CCl_2F_2 will be shifted towards Smith's data [15] and will be practically identical with those. It is interesting to note, that generally the differences between the different k_{th} shown in Fig. 4 are particular evident at elevated gas temperatures (above about 500 K).

It must be noted however, that the activation energies determined from thermal rate constants calculated from measured cross-sections (shown in the form of an Arrhenius plot in Fig. 5) are considerably smaller in comparison with those found in swarm experiments. While the typical values of AE determined by swarm experiments are close to the value of 150 meV, the value derived from the data of Kiendler et al. is 100 meV, for Handorf and Illenberger 82 meV, and for Matejčík et al. 75 meV.

It is clear, that on the one hand the accuracy of normalised absolute cross-section data directly depends on the quality of the thermal rate constant employed in the normalisation procedure. Another problem arising in this normalisation procedure is the selection of an appropriate EEDF, in particular if the mean electron energy due to the applied electric field differs from the mean energy of the gas molecules. The differences between the rate constant calculated from beam data using formula (6) in the case of a Maxwell–Boltzmann EEDF and a Druyvensteyn EEDF were discussed earlier by Chutjian [43]. In order to elucidate this problem we have compared the calculated $k_T(\langle\varepsilon\rangle, T_G)$ functions for the four sets of the attachment cross-section data [20,21,24,41] using different EEDF with the recently published experimental data measured in N_2 buffer gas with traces of CCl_2F_2 [25]. The following EEDF have been used.

- Normalised Maxwell–Boltzmann distribution function using the equivalent temperature of electrons derived from the mean electron energy.
- Functions determined for N_2 by McCorkle et al. [13] by solution of transport equation at ultra low reduced electric fields.
- Functions calculated by Nigham numerically [51], solving the Boltzmann equation for condition typical in electrical discharges.
- Functions generated by BOLSIG programme available on Internet using the two-term expansion [52].

Generally the attachment rate constant values $k_T(\langle\varepsilon\rangle, T_G)$ can be expressed as:

$$k_T(\langle\varepsilon\rangle, T_G) = \sqrt{\frac{2}{m_e}} \int_0^\infty \sigma(\varepsilon, T_G)\varepsilon^{1/2} f(\varepsilon, \langle\varepsilon\rangle T_G)\mathrm{d}\varepsilon \quad (9)$$

where $f(\varepsilon, \langle\varepsilon\rangle, T_G)$ is the EEDF function normalised to unity, also depending on the gas temperature T_G. The mean electron energy $\langle\varepsilon\rangle$ was obtained by averaging the electron energy ε:

$$\langle\varepsilon\rangle = \int_0^\infty \varepsilon f(\varepsilon, T_G)\mathrm{d}\varepsilon \quad (10)$$

In the case of a Maxwell–Boltzmann EEDF normalised to unity:

$$f(\varepsilon, T_e) = \frac{2}{\sqrt{\pi}}(k_B T_e)^{-3/2}\varepsilon^{1/2}\exp\left[-\frac{\varepsilon}{k_B T_e}\right] \quad (11)$$

the mean energy is:

$$\langle\varepsilon\rangle = \tfrac{3}{2}k_B T_e \quad (12)$$

Therefore, the equivalent electron temperature T_e was taken for each mean energy $\langle\varepsilon\rangle$ from (12) and used for the calculation of the distribution function (11). In case of the EEDF taken from [13,51,52] for nitrogen buffer gas the mean electron energy at various reduced electric fields E/N was derived by using formula (10).

The selected dependencies of attachment rate constants k_T on the mean electron energy, calculated by using formula (9) and the modified cross-sections shown in Figs. 1–3, as well as the absolute data from [20], are presented in Figs. 6–12. The calculated data are compared with experimental data measured directly at the same or very similar gas temperature by Wang et al. [25].

As it can be seen in Figs. 6–12, there exist characteristic differences between the experimentally determined rate constant data and the data calculated either by using the Maxwell–Boltzmann EEDF or the various EEDF for N_2. For instance the remarkable difference in the shape and the magnitude of calculated and experimentally measured $k_T = f(\langle\varepsilon\rangle)$ seen in Fig. 6 is most likely caused by discrimination of Cl^- ions produced via (1) at electron energies above 0.3 eV in our earlier experiment [21]. The calculated rate constant values decrease much faster with increasing electron energy than the experimental values of Wang et al. [25]. The maximum in the rate constant values observed at approximately 0.8 eV in the experimental data [25] is completely absent in the calculated values. It should be noted that in a follow up experiment to [21] by Denifl et al. [26] discrimination was reduced and an additional peak in the electron attachment cross-section at about 0.8 eV (observed already by others) has been observed.

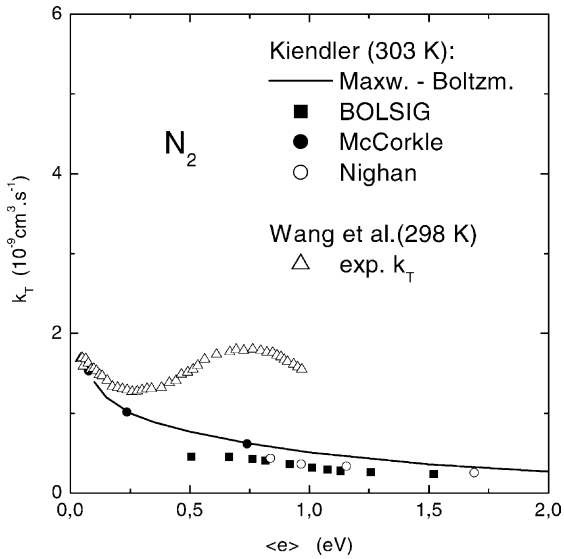

Fig. 6. Dissociative attachment rate constant for CCl_2F_2 vs. mean electron energy $\langle\varepsilon\rangle$ measured [25] and derived from cross-section [21].

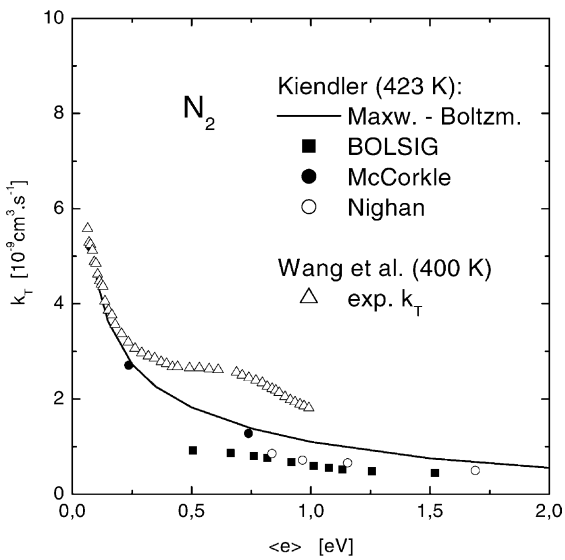

Fig. 7. Dissociative attachment rate constant for CCl_2F_2 vs. mean electron energy $\langle\varepsilon\rangle$ measured [25] and derived from cross-section [21].

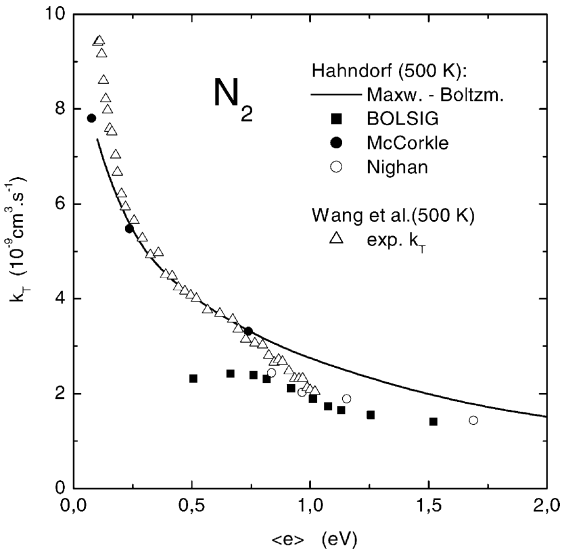

Fig. 8. Dissociative attachment rate constant for CCl_2F_2 vs. mean electron energy $\langle\varepsilon\rangle$ measured [25] and derived from cross-section [24].

The discrepancy between the calculated k_T values using the cross-section data from Kiendler et al. [21] and the measured values from Wang et al. becomes less severe at higher temperatures, e.g., see Fig. 7 showing a comparison at 423 K. An even better agreement can

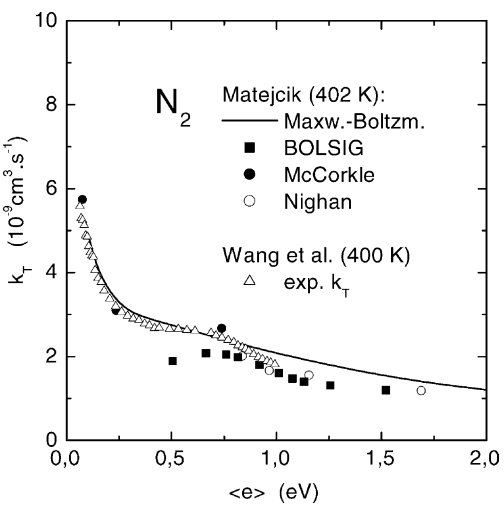

Fig. 9. Dissociative attachment rate constant for CCl_2F_2 vs. mean electron energy $\langle\varepsilon\rangle$ measured [25] and derived from cross-section [41].

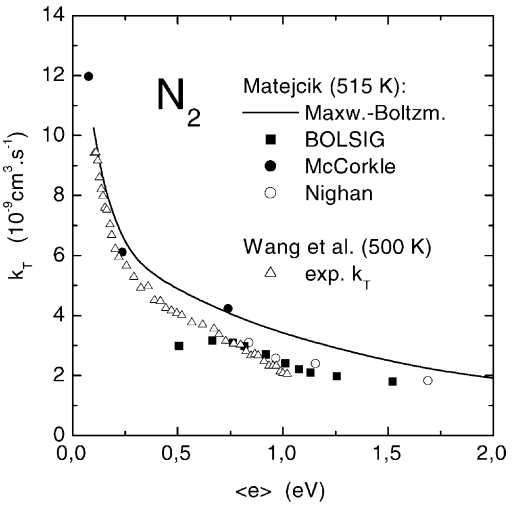

Fig. 10. Dissociative attachment rate constant for CCl_2F_2 vs. mean electron energy $\langle\varepsilon\rangle$ measured [25] and derived from cross-section [41].

be seen for the data of Handorf and Illenberger [24] shown in Fig. 8 for a temperature of 500 K. The situation for the data of Matejčík et al. [41] shown for temperatures of 402 and 515 K in Figs. 9 and 10 is similar.

In contrast to these three sets of calculated values for the rate constants using cross-section data from

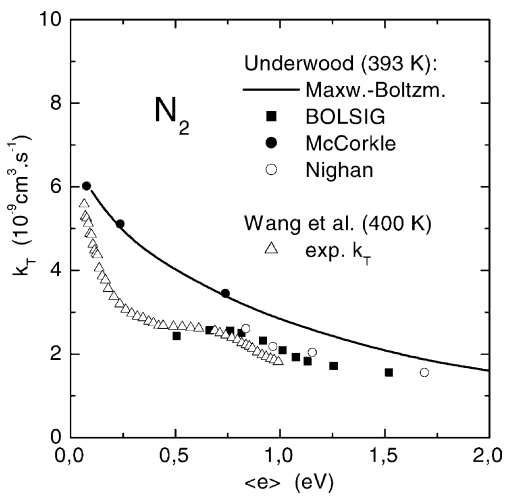

Fig. 11. Dissociative attachment rate constant for CCl_2F_2 vs. mean electron energy $\langle\varepsilon\rangle$ measured [25] and derived from cross-section [20].

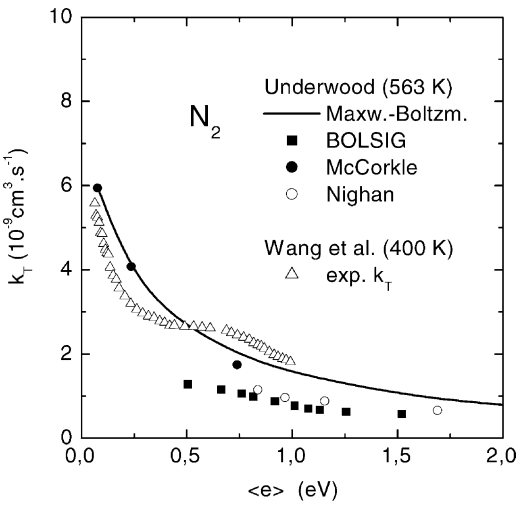

Fig. 12. Dissociative attachment rate constant for CCl_2F_2 vs. mean electron energy $\langle\varepsilon\rangle$ measured [25] and derived from cross-section [20].

[21,24,41] the k_T values calculated from the absolute cross-section data measured by Underwood-Lemons do not increase with the temperature (see Figs. 11 and 12). On the contrary the values of the rate constant calculated at $T = 563$ K are smaller than those at $T = 393$ K (see Fig. 12).

From the data presented in Figs. 6–12 one can conclude that there is general a good agreement between rate constant values calculated by Maxwell–Boltzmann distribution function and those calculated by the McCorkle EEDF [51]. The best agreement between the calculated values (using the cross-section data) and the measured k_T values of Wang et al. [25] is always seen at low electron energies. At higher mean electron energies the difference between experimental and calculated k_T is larger. For higher energy values a better agreement can be achieved by using the data generated with the BOLSIG EEDF program.

Acknowledgements

This work has been carried out within the Association EUROATOM-ÖAW. The content of the publication is the sole responsibility of its publishers and it does not necessarily represent the views of the EU Commission or its services. Partial support by the FWF, Wien, the European Commission, Brussels and of Slovak Grant Agency (Project No. 1/8313/01) is also gratefully acknowledged.

References

[1] M.J. Molina, Nature 249 (1974) 810.
[2] I.S. Buchelnikova, Soviet Phys. JETP 35 (1959) 783.
[3] T.G. Lee, J. Chem. Phys. 67 (1963) 360.
[4] L.G. Christophorou, J.A.D. Stockdale, J. Chem. Phys. 48 (1968) 1956.
[5] R.P. Blaustein, L.G. Christophorou, J. Chem. Phys. 49 (1968) 1526.
[6] W.E. Wentworth, R. George, H. Keith, J. Chem. Phys. 51 (1969) 1791.
[7] C.L. Chen, P.J. Chantry, Bull. Am. Phys. Soc. 17 (1972) 1133.
[8] K.G. Mothes, E. Schultes, R.N. Schindler, J. Phys. Chem. 76 (1972) 3758.
[9] K.M. Bansal, R.W. Fessenden, J. Chem. Phys. 59 (1973) 1760.
[10] L.G. Christophorou, D.L. McCorkle, D. Pittman, J. Chem. Phys. 60 (1974) 1183.
[11] L.G. Christophorou, Chem. Rev. 76 (1976) 409.
[12] R. Schumacher, H.R. Sprünken, A.A. Christodoulides, R.N. Schindler, J. Phys. Chem. 82 (1978) 2248.
[13] D.L. McCorkle, A.A. Christodoulides, L.G. Christophorou, I. Szamrej, J. Chem. Phys. 72 (1980) 4049.
[14] L.G. Christophorou, R.A. Mathis, D.R. James, D.L. McCorkle, J. Phys. D: Appl. Phys. 14 (1981) 1889.
[15] D. Smith, N.G. Adams, E. Alge, J. Phys. B: At. Mol. Phys. 17 (1984) 461.
[16] S.H. Alajajian, A. Chutjian, J. Phys. B: At. Mol. Phys. 20 (1987) 2117.
[17] W.C. Wang, L.C. Lee, IEEE Trans. Plasma Sci. PS-15 (1987) 460.
[18] C.J. Marotta, C. Tsai, D.L. Mac Fadden, J. Chem. Phys. 91 (1989) 2194.
[19] D. Smith, P. Spanel, Adv. At. Mol. Opt. Phys. 32 (1994) 307.
[20] T. Underwood-Lemons, T.J. Gergel, J.H. Moore, J. Chem. Phys. 102 (1995) 119.
[21] A. Kiendler, S. Matejcik, J.D. Skalny, A. Stamatovic, T.D. Märk, J. Phys. B: At. Mol. Opt. Phys. 29 (1996) 6217.
[22] S.J. Burns, J.M. Matthews, D.L. MacFadden, J. Chem. Phys. 100 (1996) 19436.
[23] J.L. Le Garrec, O. Sidko, J.L. Queffelec, S. Hamon, J.B.A. Mitchell, B.R. Rowe, J. Chem. Phys. 107 (1997) 54.
[24] I. Hahndorf, E. Illenberger, Int. J. Mass Spectrom. Ion Process. 167/168 (1997) 87.
[25] Y. Wang, L.G. Christophorou, J.K. Verbrugge, J. Chem. Phys. 109 (1998) 8304.
[26] G. Denifl, D. Muigg, I. Walker, P. Cicman, S. Matejcik, J.D. Skalny, A. Stamatovic, T.D. Märk, Czech. J. Phys. 49 (1999) 383.

[27] I. Szamrej, W. Thórzewska, H. Kość, M. Foryś, Radiat. Phys. Chem. 47 (1996) 269.
[28] Q.B. Lu, Z. Ma, T.E. Madey, Phys. Rev. B 58 (1998) 16446.
[29] Q.B. Lu, T.E. Madey, J. Chem. Phys. 111 (1999) 2861.
[30] Q.B. Lu, T.E. Madey, Phys. Rev. Lett. 82 (1999) 4122.
[31] D. Field, N.C. Jones, C.L. Lunt, J.P. Ziesel, R.J. Gulley, J. Chem. Phys. 115 (2001) 3045.
[32] Z.L. Petrovic, W.C. Wang, L.C. Lee, J. Chem. Phys. 90 (1989) 3145.
[33] S. Ushiroda, S. Kajita, Y. Kondo, in: T. Goto (Ed., Nagoya University), Proceedings of the XXVth ICPIG, Nagoya, Japan, Vol. 3, 2001, p. 257.
[34] E. Illenberger, H.U. Scheunemann, H. Baumgärtel, Chem. Phys. 37 (1979) 21.
[35] V.M. Pejčev, M.V. Kurepa, I.M. Čadež, Chem. Phys. Lett. 63 (1979) 301.
[36] L.A. Pinnaduwage, P.G. Datskos, J. Appl. Phys. 84 (1998) 3442.
[37] L.G. Christophorou, J.K. Olthoff, Y. Wang, J. Phys. Chem. Ref. Data 26 (1997) 1205.
[38] E. Illenberger, B.M. Smirnov, Phys.-Uspekhi 41 (1998) 651.
[39] L.G. Christophorou, J.K. Olthoff, Adv. At. Mol. Opt. Phys. 44 (2000) 155.
[40] J.D. Skalný, Š. Matejčík, T. Mikovíny, J. Vencko, G. Senn, A. Stamatovic, T.D. Märk, Int. J. Mass Spectrom. 205 (2001) 77.
[41] Š. Matejčík, V. Foltin, M. Stano, J.D. Skalný, Int. J. Mass Spectrom. 223–224 (2003) 9.
[42] E. Illenberger, A. Niehaus, Z. Phys. B 20 (1975) 33.
[43] A. Chutjian, Phys. Rev. Lett. 46 (1981) 1511.
[44] F.B. Dunning, J. Phys. Chem. 91 (1987) 2244.
[45] X. Ling, B.G. Lindsay, K.A. Smith, F.B. Dunning, Phys. Rev. A 45 (1992) 242.
[46] A. Chutjian, A. Garscadden, J.M. Wadehra, Phys. Rep. 264 (1996) 393.
[47] D. Klar, M.W. Ruf, H. Hotop, Aust. J. Phys. 45 (1992) 263.
[48] D. Spence, G.J. Schulz, J. Chem. Phys. 58 (1973) 1800.
[49] F.C. Fehsenfeld, J. Chem. Phys. 53 (1970) 2000.
[50] Z.L. Petrovic, R.W. Crompton, J. Phys. B: At. Mol. Phys. 17 (1985) 2777.
[51] W.L. Nighan, Phys. Rev. A 2 (1970) 1989.
[52] BOLSIG programme: http://www.kinema.com/siglo/bolsig.htm
[53] G.M.W. Kroesen, W.W. Stoffels, E. Stoffels, M. Haverlag, J.H.W.G. de Boer, F.J. de Hoog, Plasma Sources Sci. Technol. 3 (1994) 246.